Greatly Enhanced Thermal Contraction at Room Temperature by Carbon Nanotubes

*Xingyuan Shen, Christopher Viney, Changchun Wang, and Jennifer Q. Lu**

A crosslinked polyarylamide polymer exhibits novel photothermal behavior, that is, reversible giant contraction in response to near infrared irradiation in addition to normal thermal expansion. Such reversibility is seldom found in a polymeric system. Due to the amphiphilic nature of the benzocyclobutene-containing triblock copolymer precursor with polyarylamide interacting strongly with few-walled carbon nanotubes (FWCNTs), they are dispersed extremely well in the polymer solution at a loading up to at least 5 wt%. Also, strained carbon double bonds on FWCNTs can directly form covalent linkages with the benzocyclobutene groups on the polymer chains via cycloaddition. The incorporation of FWCNTs increases mechanical stiffness two-fold. Exploiting the ability of FWCNTs to effectively convert photon energy into heat and to provide conductive pathways, the NIR-induced unexpected contraction stress can be further increased dramatically. The systematic study suggests that there is an optimal CNT concentration. At 3 wt% FWCNTs, the enhancement factor for contraction stress is almost 24: 166 kPa with 3 wt% FWCNTs versus 7 kPa without FWCNTs. The colossal photothermal contraction stress generated by this new composite film at ambient condition upon NIR stimulation can lead to the development of new NIR actuators, for example, for biological applications, and create new material platforms for green energy conversion.

1. Introduction

Polymer-based stimuli-responsive systems have garnered enormous interest due to their ability to generate large volumetric or shape changes in response to various stimuli, for instance, electrically-based,[1–4] thermally driven,[5–8] or optically-driven.[9–17] Optically triggered systems are appealing due to their ability to achieve temporal and spatial control non-invasively and remotely. Over the years, moieties that can undergo conformational changes, for example, N=N,[9–15] and C=C,[16] or bond breaking, for example, spiropyran units,[17] have been incorporated into polymer systems to induce mechanical deformation. Indeed, the incorporation of photoisomerizable groups such as azobenzene entities into liquid crystal elastomers results in large mechanical deformation upon UV illumination.[13] However, in certain applications, for instance, in biomedical contexts, high-energy UV or blue photons cannot penetrate into cells and tissues. Large attenuation in air limits their actuation range and thus hinders remote applications. Furthermore, apoptosis induced by UV has been documented in some cell culture models.[18] Using such a high-energy source can degrade the polymer matrix over time. Thus, low-energy and hence less harmful near infrared (NIR) photons that penetrate tissues and have low absorption by water[19] are highly desirable stimulus sources.

NIR absorbers such as Au nanoparticles and rods and carbon allotropes have been incorporated in thermally responsive polymers to generate NIR-induced mechanical response.[20–24] For example, carbon nanotubes (CNTs) that can effectively absorb NIR photons and through non-radiative decay of absorbed infrared photons raise the internal temperature have enabled liquid crystal elastomers to undergo the disorder (NIR on) to order (NIR off) transition which is manifested by cyclic mechanical deformation.[23] A hydrogel deformation that can be triggered by NIR has been achieved by introducing Au nanoparticles, NIR absorbers, in poly(N-isopropylacrylamide) that swells below the critical transition temperature and de-swells above the critical transition temperature.[20] In addition to capturing NIR photons effectively and converting their energy into heat, these fillers have shown the ability to improve heat transfer and to enhance mechanical properties, including greatly improving recovery stress in thermally responsive material systems.[22–24] However, due to the intrinsically irreversible conformational changes associated with large-scale polymer chain rearrangement, incomplete shape recovery is often a major detrimental aspect in these stimuli-responsive materials. Furthermore, the overwhelming majority of thermally responsive polymer systems possess a transition temperature that is considerably higher than room temperature. Thus, they are not suitable for ambient-based applications.

X. Shen, Prof. C. Viney, Prof. J. Q. Lu[+]
Materials Science and Engineering
School of Engineering
University of California at Merced Merced, USA
E-mail: jlu5@ucmerced.edu
X. Shen, Prof. C. C. Wang
State Key Laboratory of Molecular Engineering of Polymers
and Department of Macromolecular Science
Laboratory of Advanced Materials
Fudan University
Shanghai, P. R. China
[+]Present address: School of Engineering, University of California at Merced, 5200 North Lake Road, Merced, CA 95343, USA

DOI: 10.1002/adfm.201301377

There are two prerequisites for a true composite system, well-dispersed filler, and strong interface. Achieving uniform heating requires these inorganic nanostructures to be evenly distributed in a polymer matrix. A cohesive interface between nanoheaters and the polymer matrix is required for minimization of loss at interfaces and ensuring that the responsive behavior is unaltered during its lifetime. In most of the reported NIR-induced responsive systems, either or both properties are intrinsically inadequate.

We have previously revealed a nanoporous crosslinked polyarylamide polymer system that can generate reversible mechanical deformation under pulsed NIR and demonstrated that the NIR-induced mechanical response remains unchanged after extended cycling.[25] We report herein that a new composite film in which pristine FWCNTs can not only disperse well in the polymer matrix at a very high loading level, that is, 5 wt%, but also form covalent linkages directly with the polymer chains. This study has revealed that FWCNTs can effectively convert photon energy into heat. The temperature increase during irradiation is 23 °C for a 3 wt% FWCNT polymer film whereas under the same power, the temperature of the pure polymer film is raised only 1 °C.

During this investigation, we have determined that the previously observed mechanical response under pulsed NIR stimulation is due to thermal expansion of the nanoporous polymer film. To our surprise, we have noticed that in addition to the normal thermal expansion due to anharmonic shape of interatomic potential, under steady NIR irradiation, this polymer generates giant anomalous thermal contraction that can be five times greater than the thermal expansion observed by fast NIR pulsing. Such contraction can be recovered after the NIR is turned off. Such reversibility has seldom been documented in a polymer system. We have found that the incorporation of FWCNTs leads to a two-fold increase of Young's modulus. Due to the excellent thermal conductivity and NIR energy absorption capability of FWCNTs, significant enhancement of mechanical response by a factor of nearly 24 for both thermal expansion and thermal contraction has been achieved comparing a 3 wt% CNT film with a pure polymer film. This new mechanically responsive composite system that harnesses synergistic interaction between FWCNTs and the new photothermal polymer material that generates contraction upon NIR stimulation can provide greatly enhanced contraction force at ambient conditions reversibly. This new platform can enable the development of new NIR based transducers for robotic maneuvering. The low-energy and less harmful NIR stimulus is compatible with biological systems and thus may be exploited for developing NIR-based pumps and valves for biological-device applications. The giant mechanical response that occurs around room temperature paves a pathway for ambient thermal energy harvesting as well as thermal energy storage.

2. Results and Discussion

2.1. Benzocylobutene-Containing Triblock Copolymer and Two Photothermal Response Components

The nanoporous polyarylamide film was formed after thermal annealing of the triblock copolymer film in which a rod-like block, polyarylamide modified with benzocylobutene (PAAM-BCB) block, is sandwiched in between two coil-like poly(ethylene glycol) (PEG) blocks. The synthetic scheme for the triblock copolymer is shown in the Supporting Information, Scheme S1. The film making procedure is described in the Experimental Section as well as Figure S1, Supporting Information, showing how to use the mold to generate uniform thin films. The thermal annealing at 350 °C removed the PEG segment according to the TGA analysis as shown in Supporting Information, Figure S2. At this temperature, close to the polymer melting temperature, BCB dimerization to crosslink polyarylamide chains will occur simultaneously.[26,27]

A tensometer was employed to characterize the NIR mechanical response of films upon stimulation. The tensile test experimental set up is shown in Figure S3 (Supporting Information, Section 1). Under constant strain, the change of stress (force) in response to NIR stimulation was measured, and simultaneously film temperature was monitored by an infrared camera. **Figure 1**a shows how the film stress (load) changes under NIR irradiation at constant strain. The consequent net contraction stress is approximately five times greater in magnitude than the net thermal expansion stress. Figure 1b contains temperature and corresponding stress as a function of time for the same film under steady NIR stimulation. Upon NIR irradiation, the initial stress drop from 1.041 MPa to 1.037 MPa at constant strain indicates that the film expands upon heating as the temperature rises from 28.3 °C to 37.0 °C. The subsequent gradual rise of stress resulting from unexpected film contraction keeps increasing even after the temperature has stabilized. Figure 1c shows stress and corresponding temperature as a function of time under rapid pulsing, that is, under 1.3 Hz NIR illumination. At fixed elongation, stress decreases due to the rapid thermal expansion and is in sync with temperature rise, whereas the increase of stress due to film contraction upon cooling is in phase with temperature drop. The difference in response to the direction of temperature change implies that the response mechanism of thermally induced contraction is different from thermally induced expansion.

Figure 2 is a plot showing the change of stress under constant strain in response to step-wise increase of power. The normal thermal expansion increases linearly with power whereas the contraction force increases greatly initially with power and then the amount of increase is diminished and finally reaches a plateau. In contrast, films that have not been annealed at 350 °C never demonstrate the unique contraction under illumination. This again suggests that the abnormal thermal contraction and the normal thermal expansion have different molecular origins. The molecular origin of the abnormal thermal contraction in the pure polymer is the subject of ongoing study.

2.2. True Composites: Well-Dispersed FWCNTs form Covalent Linkage with Polymers

To harness this novel thermal response that has never been reported before, we have employed FWCNTs to absorb NIR photons and convert them into thermal energy. It is expected that FWCNTs will provide conductive pathways to further enhance thermal response behavior. Due to the amphiphilic

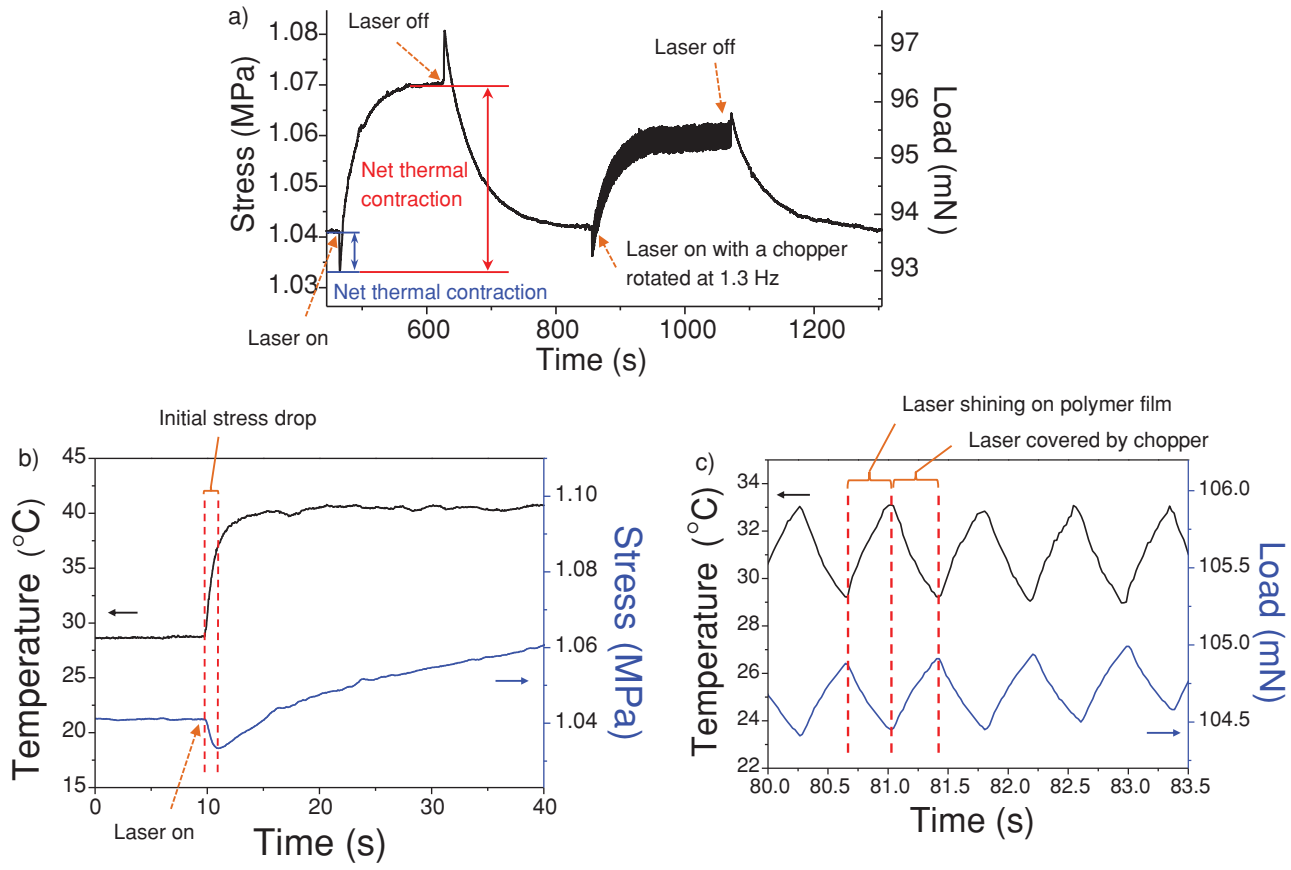

Figure 1. Tensometer data from a pure polymer film under 785 nm irradiation at a power of 42 mW. a) Stress (load) measured at constant strain upon NIR illumination without and then with a chopper rotated at 1.3 Hz, thermal expansion is highlighted in blue whereas thermal contraction is highlighted in red. b) Temperature and stress profile upon steady illumination. c) Temperature and force profile under 1.3 Hz illumination.

nature of the triblock polymer, FWCNTs can disperse very well in the triblock copolymer solution. The aromatic rod-like (PAAM-BCB) block is expected to preferentially interact with CNTs whereas the aliphatic coil-like PEG block will preferentially intermingle with the solvent, N-methyl pyrrolidone (NMP). In contrast, if only PAAM-BCB is used, aggregation in the solution of PAAM-BCB and FWCNTs can be observed within five minutes after mixing due to the strong interaction between CNTs and PAAM-BCB. **Figure 3**a is a set of optical images demonstrating that 5 wt% CNTs can disperse well in the triblock polymer solution. There is no sign of aggregation, even after 12 months.

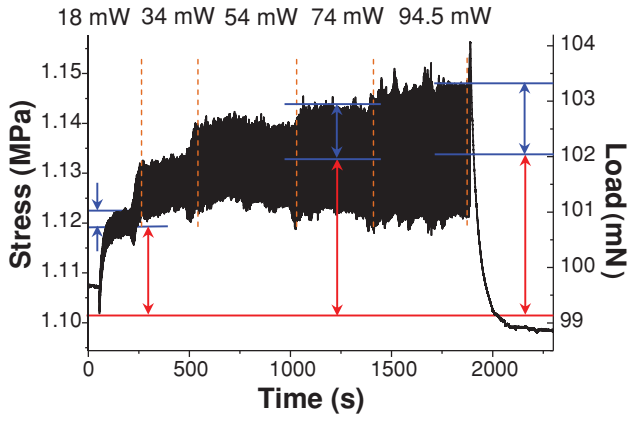

Figure 2. Tensometer measurement of a pure polymer film with different exposure power settings under 785 nm irradiation at a freqency of 1.3 Hz.

This new triblock copolymer system not only can disperse FWCNTs well but also can form strong interfaces with FWCNTs via covalent linkages. It is known that BCB groups react with conjugated CNTs via cyclo-addition.[28] To examine if this new polymer system will react with pristine CNT surfaces, FWCNTs were mixed with XTA monomer, a structural element in the rod-like PAAM-BCB block (Supporting Information, Scheme S1). The differential scanning calorimeter (DSC) analysis is displayed in Figure 3b. To facilitate detection of the reaction temperature of XTA and FWCNTs, a large excess of FWCNTs was present to avoid the dimerization of BCB in this experiment. The first-order exothermic peak with an onset temperature of 207 °C observed for the mixture of XTA and FWCNTs suggests that covalent linkages can be established between rod-like (PAAM-BCB) block and pristine FWCNT surfaces. Thus, we have evidence that a true composite in which FWCNTs are well dispersed in the polymer matrix and are connected with the polymer matrix via covalent linkages, has been created. For XTA only, the BCB dimerization temperature is 241 °C which is

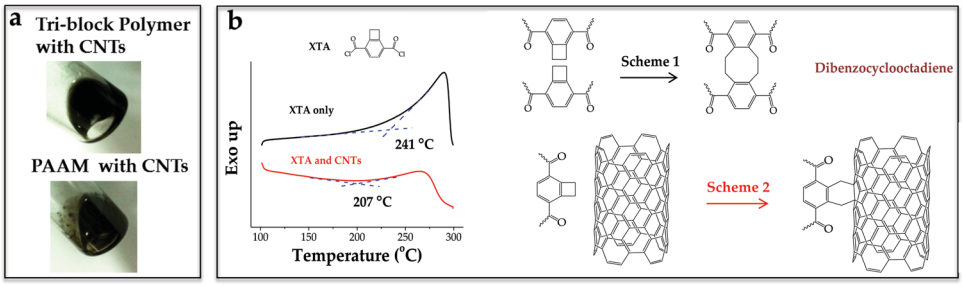

Figure 3. FWCNTs dispersion and interaction with the triblock polymer. a) Optical images of FWCNTs mixed with the triblock copolymer solution (top) and with PAAM-BCB polymer only solution (bottom). b) DSC analysis showing endothermic peaks associated with two reactions, BCB dimerization (scheme 1) and BCB and FWCNT reaction (scheme 2).

30 °C higher than the reaction temperature between FWCNTs and BCB groups. Of course, the reaction temperatures for Scheme 1 and Scheme 2 in the polymer system will take place at a temperature close to the melting temperature of PAAM-BCB that is above 300 °C and close to 350 °C.[26,27] Therefore, a true composite in which FWCNTs are well dispersed in the polymer matrix and are connected with the polymer matrix via covalent linkages, has been created.

Figure S4 (Supporting Information, Section 2) contains optical images of polymer solutions mixed with different amounts of FWCNTs and corresponding UV visible spectra. The red-shifted absorption, as well as increasing absorption, are consequence of FWCNT addition. Pure polymer and composite films have been fabricated by solution casting and then subsequent thermal annealing at a temperature up to 350 °C under argon. **Figure 4** contains a set of representative atomic force microscope (AFM) images of annealed films revealing the effect of FWCNTs on film morphology. The triblock polymer has a strong tendency to self-assemble due to high physical and chemical dissimilarity between PAAM-BCB and PEG blocks. After annealing at 350 °C, the PEG blocks are removed, resulting in nanoscale porous channels. The observed nanofilaments are crosslinked and composed of self-assembled rod-like blocks.

Comparing the AFM images of polymer films with low FWCNT loadings, that is, 0.3 and 0.5 wt% FWCNTs, with the

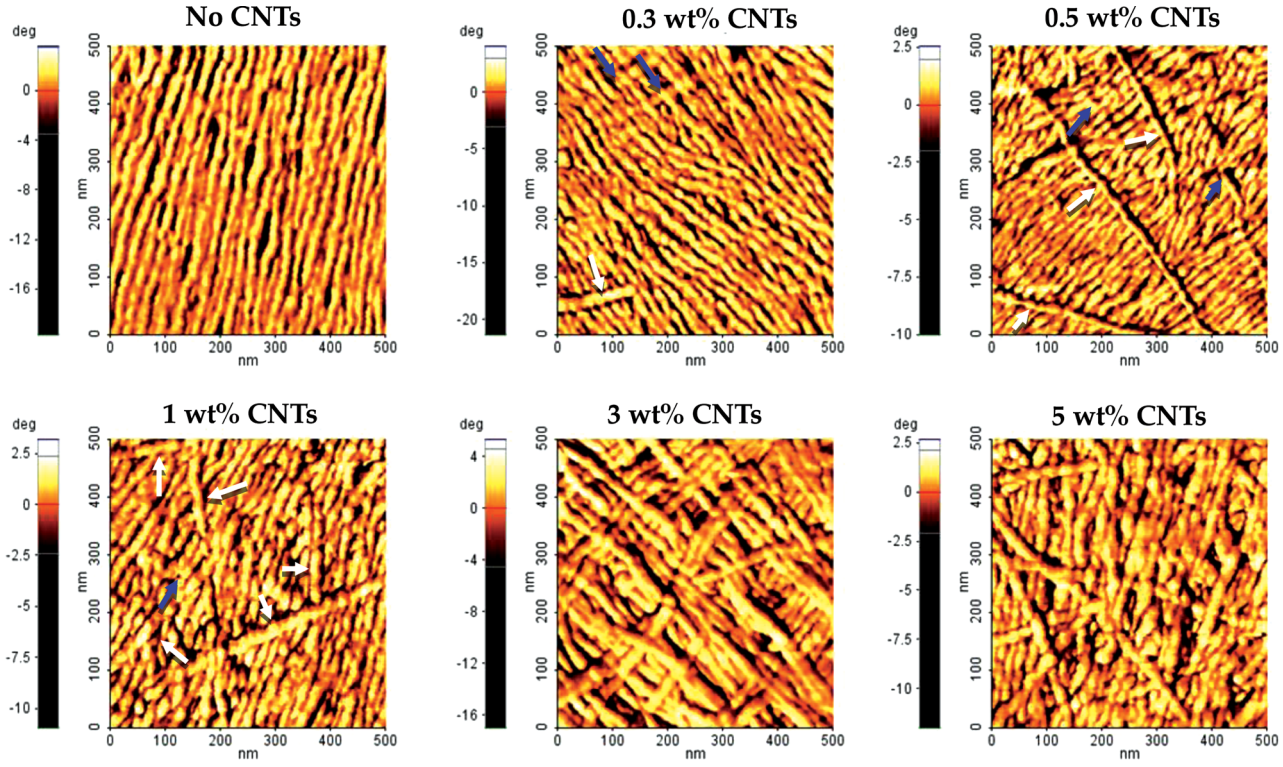

Figure 4. AFM phase images of pure polymer and polymer mixed with different amounts of FWCNTs. White arrows suggest that FWCNTs are on the surfaces and blue arrows imply FWCNTs that are below the polymer surface.

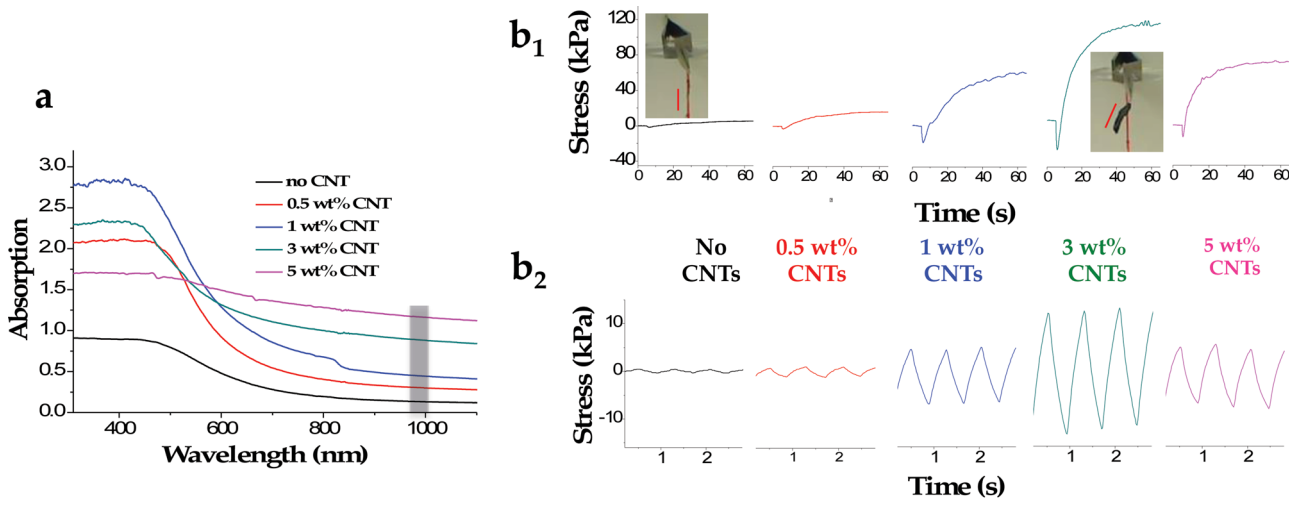

c

Film	Contraction stress (kPa) (Temperature rise (°C)) Steady illumination	Expansion stress (kPa) (Temperature rise (°C)) (1.3 Hz)
No CNTs	7.1 (1.2)	0.6(0.5)
0.5 wt% CNTs	20.0 (2.6)	3.2 (1.6)
1 wt% CNTs	80.9 (8.8)	6.0 (4.8)
3 wt% CNT	166.0 (23.8)	12.7(14.4)
5 wt% CNTs	84.6 (24.2)	6.2 (14.5)

Figure 5. Effect of FWCNTs on NIR absorption, film temperature rise and mechanical response upon a 970 nm NIR illumination at a power of 43 mW. a) UV-Vis spectra, the light absorption under 970 nm NIR illumination is highlighted in blue. b_1) Contraction stress at constant strain under steady illumination, inserts are digital camera images showing the degree of mechanical response between a no FWCNT film vs 3 wt% FWCNT films; b_2) Expansion stress of films under 1.3 Hz pulsed illumination. c) Table summarizes the net contraction stress under steady illumination and corresponding film temperature and the net expansion stress generated under 1.3 Hz illumination and corresponding film temperature as well.

AFM image of a polymer film without FWCNTs, the presence of small amounts of FWCNTs has no significant impact on the self-assembled polymer morphology. A few fibrillar structures with diameter greater than that of polymer nanofilaments have been observed for FWCNT doped films. These fibrillar structures can be reasonably assumed to be polymer encapsulated FWCNTs. Interestingly, these fibers are predominately oriented perpendicular to the axis of polymer nanofilaments. As can be seen, increasing the percentage of FWCNTs leads to the disappearance of the nanofilament structure and formation of bamboo-like morphology. At 3 wt%, a mat with cross-like morphology is observed. Adding more FWCNTs in the polymer will result in disintegration of the ordered structure as shown by the AFM phase image of the 5 wt% FWCNT film, suggesting that the bamboo-like polymer rods can be easily distinguished from single and isolated FWCNTs which are still oriented perpendicular to polymer fibers. The scanning electron microscopy (SEM) images as shown in Figure S5 (Supporting Information, Section 3), further suggest that high-loading of FWCNTs will affect the self-assembly of polymer chains, corroborated by the AFM results. The ability of FWCNTs to alter the self-assembled polymer morphology is another valuable evidence that there is a strong interaction between FWCNTs and the polymer.

UV-Vis spectra of suspended films with and without FWCNTs after annealing at 350 °C are displayed in **Figure 5**a. As expected, the higher percentage of FWCNTs results in more absorption in the NIR region. The effect of adding FWCNTs in films is similar to that in solution when the FWCNT concentration is about 1 wt% or less. However, the reduction of the polymer absorption peak in the UV region and the broadening of the absorption band in the visible region under FWCNT loading, for example, 3 wt% and 5 wt%, further suggests that FWCNTs interact strongly with the polymer, especially in the film format. Thermal images under steady 970 nm irradiation at 43 mW can be found in Figure S6a (Supporting Information, Section 3). The temperature rise for 3 wt% and 5 wt% FWCNT films is similar. Figure S6b, Supporting Information, shows that 1.69% of incident 970 nm radiation is transmitted by a 15 micrometer thick 3 wt% FWCNT film whereas 0.67% is transmitted using a 5 wt% FWCNT film. Therefore, 3 wt% FWCNTs in a 15 micrometer thick film is sufficient to absorb almost all NIR photons. The enlarged heated area with increasing CNT content indicates that adding FWCNTs enhances thermal conductivity.

Young's modulus is calculated from a load versus extension curve and displayed in Figure S7 (Supporting Information, Section 3). At 3 wt% FWCNTs, Young's modulus of the

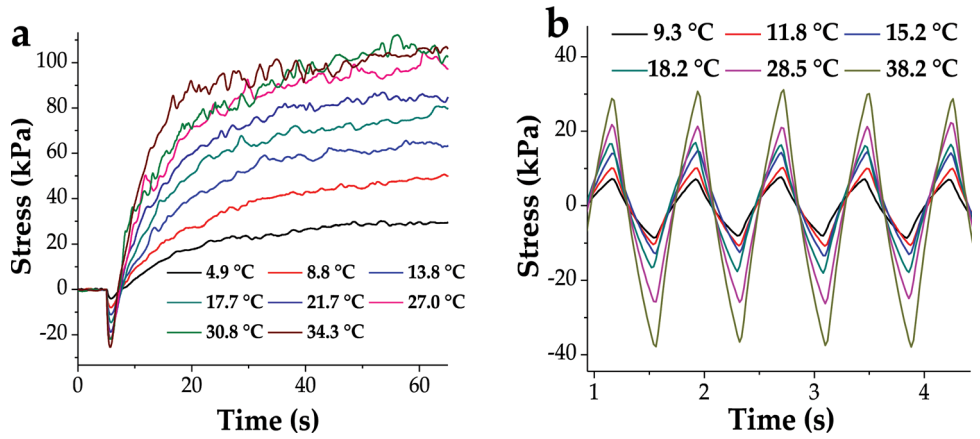

Figure 6. Tensometer data of a film with 3 wt% FWCNTs under different laser power settings using a 970 nm laser to heat the film, the temperatures shown in the figures are the temperature increases, i.e., differences between the room temperature and film temperatures. a) Contraction stress of films under steady illumination at different temperature rise. b) Expansion stress of films under a 1.3 Hz pulsed illumination at different temperature rise.

polymer film is nearly twice that of the pure polymer film. The observed mechanical property enhancement can be attributed to the combination of excellent FWCNT dispersion and strong interface bonding. The decrease of Young's modulus value at 5 wt% loading might be caused by a reduction of intermolecular bonding as more BCB groups are consumed by reaction with CNTs.

2.3. Comparison of NIR-Induced Mechanical Response Under Constant Power

For side-by-side comparison of the effect of CNTs on the NIR-induced mechanical response behavior, a nominal preload of 0.1 N (the results are not sensitive to this value) was first applied to all films under investigation. Net contraction stress under steady illumination is displayed in Figure 5b$_1$, whereas the net thermal expansion stress under short NIR pulsing (1.3 Hz) is shown in Figure 5b$_2$. Figure 5c is a table that summarizes the magnitude of contraction stress and expansion stress generated by films that contain different amounts of CNTs, along with the corresponding temperature rise. Values listed in Figure 5c are directly obtained from Figure 5b$_1$,b$_2$. At each FWCNT concentration, a couple of films have been tested. Very similar results at each concentration have been obtained. Because of strong NIR absorption, the amount of generated contraction stress rises significantly with the increase of FWCNT content. Comparing a pure polymer film with a 3 wt% FWCNT film under a 970 nm laser illumination at a power of 43 mW, the generated contraction stress is enhanced 24 times, 166 kPa (3 wt%) versus 7 kPa (no FWCNTs). This significant enhancement is because the rise in temperature for the 3 wt% FWCNT-polymer film is about 23 °C whereas the temperature increase of the pure polymer film is only 1 °C under the same irradiation power. Similarly, under 1.3 Hz pulsed NIR irradiation, the generated expansion stress is also increased greatly, by approximately 20 times. Incorporation of FWCNTs that can effectively absorb NIR and increase thermal conductivity can significantly enhance energy transduction between NIR photothermal or thermal energy and mechanical energy.

There is an optimal FWCNT concentration. Excessive FWCNTs, for example, beyond 5 wt%, will not further increase film temperature rise. We propose that increasing FWCNT concentrations result in more BCB groups in the polymer being consumed by reaction with strained carbon-carbon double bonds on the surfaces of FWCNTs. This will result in less extent of crosslinking between polymer chains. FWCNTs can also act as nanoscale barriers to prevent mechanical deformation and recovery. Together with the disruption of ordered nanofilament morphology, these considerations can explain the deterioration of NIR-induced mechanical response when the FWCNT concentration is too high, for instance, the 5 wt% FWCNT film yields less contraction stress than the 3 wt% FWCNT film.

The cycle performance test shown in Figure S8 (Supporting Information, Section 3), indicates that the abnormal thermal contraction is recoverable. Therefore the possibility that an internal state formed during film processing is the origin of the observed unusual thermal contraction can be ruled out. The excellent cycle performance is in part attributed to the lack of soft components and use of low-energy NIR stimulus.

To further investigate thermal contraction behavior, the generated contraction stress under steady NIR exposure at different laser power settings was measured and concomitantly film temperature was recorded. The generated contraction stress in response to film temperature rise, obtained by adjusting laser power, is displayed in **Figure 6**a. Analogously, the thermal expansion stress obtained by 1.3 Hz pulsed NIR stimulation as a function of film temperature rise, is displayed in Figure 6b. There is almost no change in contraction force from ΔT = 30.8 °C to ΔT = 34.8 °C, implying that an equilibrium has been reached. In contrast, thermal expansion force due to anharmonic thermal oscillation in an asymmetric potential increases linearly with temperature. The contraction force reaches a plateau indicating that the contraction may result from a previously unidentified molecular level conformational change.

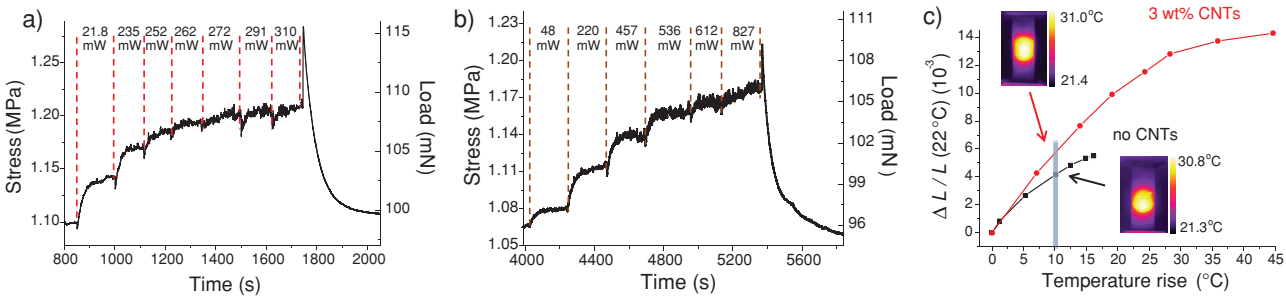

Figure 7. Thermal contraction of films with and without CNTs under 970 nm illumination. a) Rising contraction due to stepwise increase in laser power for a 3 wt% FWCNT film, b) Rising contraction due to stepwise increase in laser power for pure polymer film, c) Contraction degree (ppm) ($\Delta L/L$ at 22 °C) as a function of temperature rise for 3 wt% FWCNT and pure polymer films; snapshot of thermal images for both films with a temperature rise of 10 °C under NIR irradiation are included.

2.4. Negative Thermal Expansion

To estimate film thermal contraction coefficient, the thermal contraction as a function of temperature rise in response to a stepped increase of laser power under constant strain was measured. **Figure 7**a,b are the representative results obtained from a 3 wt% FWCNT film and pure polymer film respectively. The thermal expansion per degree for 3 wt% composition film was calculated to be -1268 ± 81 ppm K^{-1} whereas the thermal expansion per degree for pure polymer films was -1215 ± 68 ppm K^{-1}. The detailed calculation is described in Supporting Information, section 4. We did the same calculation for 0.5 wt% FWCNT films (Figure S10, Supporting Information). The thermal expansion per degree for the 0.5 wt% composition films was calculated to be -1301 ± 50 ppm K^{-1}. As expected, the thermal response, that is, thermal contraction per degree, is very similar comparing pure polymer films to 3 wt% and 0.5 wt% composite films. This result suggests FWCNTs themselves do not contribute to thermal contraction. Figure 7c shows thermal contraction per degree as a function of temperature for films with 3 wt% FWCNTs (Figure 7a) and without FWCNTs (Figure 7b). The fact that the maximum strain increases greatly with the addition of FWCNTs can be attributed to thermal conductivity (more area are heated and thus stimulated) as well as improved mechanical properties.

2.5. Comparison of NIR-Induced Mechanical Response at the Same Temperature Rise

The influence of CNTs on NIR-induced mechanical response was further evaluated by comparing the generated contraction stress in response to 10 °C temperature rise. As shown in Figure S9 (Supporting Information, Section 3), a 1 wt% FWCNT film can generate 75 kPa contraction stress whereas a pure polymer film can only produce 17 kPa. On one hand, CNTs improve film mechanical integrity and also increase heated volume of a polymer film because of improved thermal conductivity. Consequently, more material will participate in the mechanical response. On the other hand, FWCNTs reduce polymer connectivity as more BCB groups will be consumed by reacting with FWCNTs and fewer are available for polymer crosslinking. Moreover, excess CNTs can hinder polymer mechanical deformation. We propose that, due to these two competing factors, 1 wt% FWCNT film provides the highest thermal contraction per degree.

3. Conclusions

A new true composite in which FWCNTs are uniformly dispersed and form covalent linkages with a novel stimuli-responsive polymer matrix has been developed. By combining the ability of FWCNTs to effectively convert photon energy into thermal energy with the NIR-induced photothermal responsiveness of the polymer, a new actuating system is introduced that can generate reversible and anomalously large contraction under NIR stimulation. This systematic investigation indicates that a nearly 24 times greater mechanical output can be achieved using a 3 wt% FWCNT film at a given power, compared to the pure polymer. The FWCNT concentration to attain the maximum NIR-induced mechanical response for a given temperature rise, for example, 10 °C is 1 wt%. This result highlights the importance of the interaction between FWCNTs and polymer on composite macroscopic performance.

Unlike most thermally responsive polymers that need either substantial amounts of thermal energy or harmful high-energy photons to induce mechanical response and often do not exhibit complete shape recovery, the new composite material described above can generate anomalous contraction upon NIR irradiation or heating a few-degrees above room temperature. In addition, only the top surface of most photoresponsive polymers can participate in mechanical deformation due to high absorption of UV photons. This new composite film exploits excellent NIR photon absorbing capability and superior thermal conductivity so that the entire thickness of the film will take part in the generation of mechanical response. Thus high performance NIR-based actuators that provide adequate energy conversion or force output otherwise unattainable can be created such as NIR micro-pumps for biological related applications. The thermal and photothermal energy transduction capability of this new composite material platform offers a new avenue for ambient thermal and NIR energy conversion and thermal fuel storage as well.[29]

4. Experimental Section

Materials Preparation: XTA was a terephthalic acid derivative with a benzocyclobutene group (acquired from Prof. David Martin at the University of Delaware). Few-walled carbon nanotubes (FWCNTs) were provided by Prof. J. Liu at Duke University. Mono-amine terminated polyethylene glycol (Mn = 2000) was purchased from Huntsman and used without any purification. 4,4′-oxydianiline (99%) was purchased from Sigma-Aldrich and used as received. Other reagents and solvents were used as received from Aldrich.

Synthesis and Characterization of Triblock Copolymer: The synthesis scheme is shown in the Supporting Information, Section 1. Triblock copolymer was synthesized by condensation of diacid chloride terminated polyarylamide (PAAM-BCB), with an excess of mono-amine terminated polyethylene glycol (PEG). PAAM-BCB was synthesized by condensation of an excess of XTA, with 4,4'-oxydianiline (ODA). First 1.5 mL of anhydrous N-methyl-2-pyrrolidone (NMP) was added into a flask containing 1.2 mmol XTA. After XTA completely dissolved in NMP, the solution was cooled down to 0 °C in an ice bath. 1.0 mmol ODA in 1.5 mL NMP solution was transferred into the XTA solution with a syringe under nitrogen protection in an ice bath. The reaction time was set to be 2 h. An excess of mono-amine terminated PEG in toluene was then added into the solution of PAAM-BCB in an ice bath. The bath temperature was then raised to 80 °C. After refluxing at 80 °C for 12 h, the solution was allowed to cool to room temperature and the triblock copolymer was collected by filtration and excess PEG was removed by washing with water and followed by tetrahydrofuran (THF) rinse. TGA (TA instruments SDT Q series) was performed (under N_2 at a heating rate of 10 °C min^{-1}) to verify the formation of block copolymers.

Formation and Characterization of CNT-Polymer Solution: To render sufficient solubility of CNTs in NMP, FWCNTs were functionalized with 4 M HNO_3. First FWCNTs were added to a 4 M HNO_3 solution and dispersed in the solution via sonication for 30 min. After refluxing at 120 °C for 48 h, FWCNTs were rinsed with water until the pH of the solution was 7. The residual water was removed by drying in an oven at 100 °C overnight and the dried acid-treated FWCNTs were then dissolved in NMP. After sonication overnight, the FWCNT suspension was centrifuged for 1 h at 8000 rpm. The precipitate, bundled FWCNTs, was removed, dried, and weighed for calculation of the CNT concentration in the FWCNT solution. After mixing a high concentration polymer solution (60 mg mL^{-1}) with different amounts of the FWCNT solution first, the FWCNT-polymer dispersions were then diluted with appropriate amounts of NMP so that all the solutions have the same polymer concentration (40 mg mL^{-1}) but different CNT concentration. UV spectrophotometer (SHIMADZU UV-Vis-NIR 3600 spectrometer) was used to record the spectra of polymer solutions. DSC (TA Q2000) was performed (under N_2 at a heating rate of 10 °C min^{-1}) to study possible chemical reactions.

Formation and Characterization of CNT-Polymer Films: Silicon substrates coated with 100 nm of thermally grown oxide were cleaned by treatment with a freshly prepared "piranha" solution (3/1, v/v, concentrated H_2SO_4/30% aqueous H_2O_2) at 90–100 °C for 1 h and then rinsed with deionized water. 110 µL of each CNT-polymer solution (40 mg mL^{-1}) was poured on a clean substrate on which a clamped custom molded Teflon frame was attached, as shown in Figure S1, Supporting Information. After air drying, the fixture and Teflon mold was removed. Then the film was annealed at 350 °C under partial vacuum with a directional flow of technical grade argon gas in a tube furnace to yield a final film thickness of approximately 15 µm. The exact same sample preparation technique was used to generate isotropic films for all the samples that were tested.

Film thickness was measured as follows: A sheet of weighing paper was folded in half, and the film was sandwiched inside this folded sheet. A micrometer (Mitutoyo Digital Micrometer, model 193–111, resolution 0.001 mm) was used to measure the thickness of the sandwich at several (at least 5) locations. The thickness of two layers of the weighing paper, that is, with no film present, was also performed at several locations. From these measurements, the film thickness was calculated. Typical values for film thickness are 15 ± 2 µm. The validity and accuracy of the measurement technique was corroborated by using a microscope equipped with a high resolution (small depth of field) objective to focus on the top and bottom surfaces of the film at several locations. Feeler gauges (thin metal foils that have an accurately known thickness) placed on the sample stage were used to calibrate the corresponding rotations of the fine-focus knob in terms of vertical stage translation and thus sample thickness.

Atomic force microscope (AFM, XE-100, Park system) and scanning electron microscope (SEM, Hitachi S-4800) were utilized to observe the morphology of films. Then films were peeled off in a buffered hydrofluoric acid solution. UV spectrophotometer (SHIMADZU UV-Vis-NIR 3600 spectrometer) was carried out to characterize the light absorption of films with different amounts of FWCNTs.

NIR Mechanical Response Characterization of CNT-Polymer Film: The CNT-polymer film was cut into a uniform 2.0 cm × 0.5 cm film and held by supergluing (Loctite Super Glue Liquid Professional) the ends between a pair of washers (18/8 stainless steel, 1/2" outer diameter, 15/64" inner diameter.). The top end of the sample was attached to a 0.5 N cantilever load cell (Model S-100, Strain Measurement Devices, Bury-St-Edmunds, UK) via a hook passing through the hole in the washers and connected to the load cell, and the lower end was secured by clamping the washers at that end in a mechanical grip. The load cell was calibrated prior to every set of measurements (i.e. every day that the equipment was used) by suspending a known mass from the load cell and using Instron Bluehill 2 software to implement the calibration. After a preload of 0.1 N (pressure equals to 1.11 MPa) was applied to the film, a laser source was used to illuminate it as indicated in Figure S3, Supporting Information. A tensometer (3369 Instron Tensile Tester) was employed to record the mechanical response of films while an infrared camera (FLIR SC645) was used to record temperature and take thermal images. A powermeter (ThorLabs S142C Integrating Sphere Photodiode Power Sensor, 350–1100 nm, connected to a ThorLabs PM100D Compact Power and Energy Meter Console) was utilized to measure the power of laser lamps. We have done 3–4 measurements for each composition. All the mechanical results in this manuscript were chosen to be representative.

Supporting Information

Supporting Information is available from the Wiley Online Library or from the author.

Acknowledgements

The authors are grateful to David C. Martin at University of Delaware for providing XTA (prepared by Gary Spilman, Ken Walker and Larry Markoski in the lab of Jeff Moore at the University of Michigan), and J. Liu at Duke University for providing FWCNTs. Financial support from DARPA(N66001-09-1-2088), CITRIS, National Science and Technology Key Project of China (Grant No. 2012AA020204) and NSFC (Grant No. 21034003) is acknowledged. The author affiliations and Figure 7 were corrected on August 23, 2013.

Received: April 23, 2013
Revised: July 3, 2013
Published online: July 31, 2013

[1] R. Shankar, T. K. Ghosh, R. J. Spontak, *Soft Matter* **2007**, *3*, 1116.
[2] R. Pelrine, R. Kornbluh, Q. B. Pei, J. Joseph, *Science* **2000**, *287*, 836.
[3] C. E. Chang, V. H. Tran, J. B. Wang, Y. K. Fuh, L. W. Lin, *Nano Lett.* **2010**, *10*, 726.

[4] T. Bailey, J. E. Hubbard, *J. Guid. Control Dynam.* **1985**, *8*, 605.
[5] Y. Y. Liu, C. M. Han, H. F. Tan, X. W. Du, *Mater. Sci. Eng. A* **2010**, *527*, 2510.
[6] J. W. Cho, Y. C. Jung, Y. C. Chung, B. C. Chun, *J. Appl. Polym. Sci.* **2004**, *93*, 2410.
[7] B. R. Ratna, D. L. Thomsen, P. Keller, J. Naciri, R. Pink, H. Jeon, D. Shenoy, *Macromolecules* **2001**, *34*, 5868.
[8] H. G. Schild, *Prog. Polym. Sci.* **1992**, *17*, 163.
[9] Y. L. Yu, M. Nakano, T. Ikeda, *Nature* **2003**, *425*, 145.
[10] T. Yoshino, M. Kondo, J. Mamiya, M. Kinoshita, Y. L. Yu, T. Ikeda, *Adv. Mater.* **2010**, *22*, 1361.
[11] M. Yamada, M. Kondo, J. I. Mamiya, Y. L. Yu, M. Kinoshita, C. J. Barrett, T. Ikeda, *Angew. Chem. Int. Ed.* **2008**, *47*, 4986.
[12] T. Ikeda, M. Nakano, Y. L. Yu, O. Tsutsumi, A. Kanazawa, *Adv. Mater.* **2003**, *15*, 201.
[13] H. Finkelmann, E. Nishikawa, G. G. Pereira, M. Warner, *Phys. Rev. Lett.* **2001**, *87*, 015501.
[14] M. Camacho-Lopez, H. Finkelmann, P. Palffy-Muhoray, M. Shelley, *Nat. Mater.* **2004**, *3*, 307.
[15] T. J. Bunning, T. J. White, S. V. Serak, N. V. Tabiryan, R. A. Vaia, *J. Mater. Chem.* **2009**, *19*, 1080.
[16] A. Momotake, T. Arai, *Polymer* **2004**, *45*, 5369.
[17] Q. A. Jin, G. Y. Liu, J. A. Ji, *J. Polym. Sci.: Polym. Chem.* **2010**, *48*, 2855.
[18] P. Kamarajan, C. C. K. Chao, *Bioscience Rep.* **2000**, *20*, 99.
[19] R. Weissleder, *Nat. Biotechnol.* **2001**, *19*, 316.
[20] Q. S. Wei, J. Ji, J. C. Shen, *Macromol. Rapid Comm.* **2008**, *29*, 645.
[21] B. P. Timko, T. Dvir, D. S. Kohane, *Adv. Mater.* **2010**, *22*, 4925.
[22] K. C. Hribar, R. B. Metter, J. L. Ifkovits, T. Troxler, J. A. Burdick, *Small* **2009**, *5*, 1830.
[23] L. Q. Yang, K. Setyowati, A. Li, S. Q. Gong, J. Chen, *Adv. Mater.* **2008**, *20*, 2271.
[24] H. Koerner, G. Price, N. A. Pearce, M. Alexander, R. A. Vaia, *Nat. Mater.* **2004**, *3*, 115.
[25] G. Ugur, J. Chang, S. Xiang, L. Lin, J. Lu, *Adv. Mater.* **2012**, *24*, 2685.
[26] K. A. Walker, L. J. Markoski, G. A. Deeter, G. E. Spilman, D. C. Martin, J. S. Moore, *Polymer* **1994**, *35*, 5012.
[27] E. Pingel, L. J. Markoski, G. E. Spilman, B. J. Foran, J. A. Tao, D. C. Martin, *Polymer* **1999**, *40*, 53.
[28] G. Sakellariou, H. Ji, J. W. Mays, N. Hadjichristidis, D. Baskaran, *Chem. Mater.* **2007**, *19*, 6370.
[29] A. M. Kolpak, J. C. Grossman, *Nano Lett.* **2011**, *11*, 3156.